



Research Article

# Combined Use of Polymers and Porous Materials to Enhance Cinnarizine Dissolution

Maryam Maghsoodi<sup>1\*</sup>, Fatemeh Shahi<sup>1</sup>

<sup>1</sup>Drug Applied Research Center and Faculty of Pharmacy, Tabriz University of Medical Sciences, Tabriz, Iran.

## Article Info

### Article History:

Received: 29 October 2018

Revised: 3 March 2019

Accepted: 30 May 2019

ePublished: 20 December 2019

### Keywords:

-Precipitation inhibitors

-Cinnarizine

-Aerosil

-Mesoporous

## ABSTRACT

**Background:** Loading of poorly water-soluble drugs on the porous materials has attracted great interest as an effective approach for enhancement of dissolution rate of drugs. The Aerosil (Ae) with porous structure is expected to facilitate the dissolution of drugs which is generally associated with precipitation. Thus, the purpose of this investigation was thus to develop a formulation which combines a precipitation inhibitor and a poorly soluble drug loaded Ae.

**Methods:** A poorly water-soluble drug, Cinnarizine (CNZ) was used as a model, and Eudragit L100 (Eu) was used as a precipitation inhibitor. Formulations were produced by solvent evaporation and characterized by FT-IR and differential scanning calorimetry (DSC). Dissolution experiments were carried out in phosphate buffer (pH 6.8) under non-sink conditions.

**Results:** DSC thermograms revealed that no crystalline structure of CNZ was present in CNZ-loaded Ae formulations and no long-range order was arranged upon loading of CNZ into Ae. In dissolution test, the CNZ-loaded Ae physically blended with Eu achieved a remarkably higher CNZ concentration over the plain CNZ and over the CNZ-Eu co-loaded Ae. The dissolution rate of CNZ from the CNZ-loaded Ae was enhanced with increasing Ae amount and the dissolution was maximum when the ratio of CNZ: Ae was 1:10 CNZ: Ae. In addition, the precipitation inhibition was increased when the amount of Eu was high.

**Conclusion:** The results of this work revealed that the dissolution behaviour of CNZ-loaded Ae is enhanced by physically blending of Eu as a suitable precipitation inhibitor.

## Introduction

Recently, mesoporous silica materials have gained much attention as a drug carrier due to their large pore volume and surface area and consequently high drug loading ability.<sup>1-4</sup> Various investigations have shown that restricting a drug to the pores of silicates resulted in amorphization. Moreover, these amorphous formulations demonstrate good physical stability with no significant change in amorphous state even at high temperature/relative humidity.<sup>5-6</sup> Following contact with dissolution medium, the restricted amorphous drug releases out of the pores. Many previous studies have shown the ability of mesoporous silicates in increasing the dissolution rate of poorly water-soluble drugs.

It has been shown that dissolving the drug in its amorphous state in the gastrointestinal tract may not be adequate for improving *in vivo* absorption, as fast precipitation to a crystalline form of the drug with less solubility may occur.<sup>7-10</sup>

Accordingly, no strong correlation was found between the dissolution rate enhancement and *in vivo* absorption improvement and only a few studies have demonstrated an increased *in vivo* absorption. The possible reason for the absence of this correlation is that unlike solid

dispersion, the mesoporous silicates have no ability to inhibit precipitation of a drug after releasing from their pores. Therefore, the presence of a polymer is necessary to stabilize the supersaturated solubility which is important for improving *in vivo* absorption. Van Speybroeck *et al.* (2010)<sup>11</sup> showed that drug loaded silica and a precipitation inhibitor polymer together increased the dissolution rate with a concomitant *in vivo* absorption improvement. The major aim of this study was to develop an amorphous formulation composed of drug loaded silica and a precipitation inhibitor. The precipitation inhibitors used in this study was Eudragit L100 (Eu). The selection of this polymer was based on the results of a previous supersaturation experiment carried out in our laboratory, indicating that, out of a wide range of polymers, only Eu was capable of preventing CNZ precipitation. Formulations were prepared by physically blending CNZ-loaded Ae with Eu or by CNZ-Eu co-loading Ae and then were evaluated by means of *in vitro* dissolution tests.

## Materials and Methods

### Chemicals

Cinnarizine was acquired from Osvah Pharmaceutical Co (Iran). Aerosil®200 (Degussa, Germany), and Eudragit

\*Corresponding Author: Maryam Maghsoodi, E-mail: maghsoodim@tbzmed.ac.ir

©2019 The Authors. This is an open access article and applies the Creative Commons Attribution (CC BY), which permits unrestricted use, distribution and reproduction in any medium, as long as the original authors and source are cited. No permission is required from the authors or the publishers.

L100 (Evonik GmbH, Germany) were purchased. Monobasic potassium phosphate USP-standard ( $\text{KH}_2\text{PO}_4$ ), dibasic potassium phosphate ( $\text{K}_2\text{HPO}_4$ ) ethanol analytical grade (Merck, Germany) were also used.

### **Supersaturation experiment**

The total time of supersaturation test was 2 h, and the buffer solution was kept in a water bath shaker at  $37 \pm 0.5$  °C at 100 rpm.

A stock solution of CNZ was prepared by dissolving 10 mg of CNZ in 10 ml HCl solution (0.1N). 1 ml of this solution was then added to 50 ml buffer solution (pH 6.8) containing 20 mg of excipient (Eu or Ae) to induce an initial drug solution concentration of 20 µg/ml CNZ, corresponding to a supersaturation ratio of 10. The total time of supersaturation test was 2 h, and the buffer solution was kept in a water bath shaker at  $37 \pm 0.5$  °C at 100 rpm. After adding HCl solution to the buffer solution, samples were taken at predetermined time points (10, 20, 30, 60 and 120 min) by withdrawing 1 ml from each vessel; then the aliquots were filtered using a nylon membrane syringe filter (0.45 µm). The obtained filtrate was directly diluted in buffer solution to avoid CNZ precipitation and analyzed using UV-Vis spectrophotometer (UV-160A, Shimadzu, Kyoto, Japan) at 253 nm. The concentration of CNZ ( $n = 3$ ) was plotted as a function of time. No interference from the excipients on the CNZ assay was detected at 253 nm.

### **Solubility**

The equilibrium solubility of CNZ was determined in phosphate buffer (pH 6.8) at 37°C using an excess of CNZ, in the presence of Eu and Ae (concentration of 0.4 mg/ml). The solubility was determined after 48 h by using UV-Vis spectrophotometer at 253 nm following filtration through a 0.45µm nylon membrane syringe filter.

### **Preparation of solid formulations**

Preparation of CNZ loaded Ae was carried out by a rotary evaporation method. First, CNZ was dissolved in ethanol (10 ml), and then a certain amount of Ae was suspended in the solution and ultrasonicated for 30 min. Then, the solution was mixed for 1 h under magnetic stirring and then the mixture was introduced into a flask and the solvent removal was performed by rotary evaporation. After that, the obtained powder was dried in a vacuum oven overnight at 40 °C to take away any remaining solvent and subsequently was grounded with a mortar and pestle and then sieved to separate a particle size fraction of 150-250 µm. In the case of CNZ-Eu co-loaded Ae samples, a certain amount of Eu was added into CNZ solution in ethanol and then the procedure was continued as explained above. Physical mixtures (PM) of CNZ loaded Ae and Eu were also prepared by weighing out the accurate amount of CNZ loaded Ae and Eu and triturating for at least 10 min in the mortar and pestle.

### **In vitro dissolution studies**

Dissolution experiment was conducted using the USP II paddle method. Samples equivalent to 20 mg of CNZ were calculated, weighted and added to each vessel. This amount of drug represented a theoretical 20 µg/ml CNZ concentration for the dissolution testing which corresponds to a 10-fold level of supersaturation supposing an equilibrium solubility of 2 µg/ml in neutral medium. Samples were subjected to a neutral medium (pH 6.8, 1000 ml) for 3h. The dissolution medium was stirred at 100 rpm and held at  $37 \pm 0.5$  °C throughout the experiment. Samples were taken at pre-determined time points by withdrawing 5 ml from vessels; then the aliquots were filtered using a nylon membrane syringe filter (0.45 µm, Whatman, Florham Park, NJ). In the meantime, an equal volume of the same medium was added to maintain a constant volume. Filtered samples were immediately diluted in a 1:1 ratio with the buffer solution (pH 6.8) to avoid drug precipitation. CNZ concentrations were assessed as mentioned above.

### **Fourier transform infrared (FT-IR) spectroscopy**

Fourier-transform Infrared (FTIR) Spectroscopy was carried out using a Spectrometer (M-B-100, Bomem, Canada) (32 scans at 4  $\text{cm}^{-1}$  resolution). The samples were mixed with KBr, compressed into a disc, and analysed directly over a wavenumber range of 400–4000  $\text{cm}^{-1}$ .

### **Differential scanning calorimetry (DSC)**

DSC analyses of the samples were performed using an automatic thermal analyzer system (DSC-60, Shimadzu, Tokyo, Japan). Samples were weighed to 5 mg in aluminum crimped pans and heated with a heating rate of 10°C/min from 25 to 300°C. Indium as standard was used to calibrate temperature.

### **Statistical evaluation of data**

The data were reported as the mean  $\pm$  standard deviation (SD). Statistical analysis was performed using the analysis of variance (ANOVA) followed by post-test with statistical significance evaluated at  $P < 0.05$ .

## **Results and Discussion**

### **Evaluation of the effect of Eu and Ae on drug supersaturation**

Inhibitory effect of Ae and Eu on CNZ precipitation was examined by assessing the maintenance ability of CNZ concentration after the creation of supersaturated solution of CNZ.

In the supersaturation test, Ae and Eu were pre-dissolved at a concentration of 0.04% w/v in buffer solution, and an aliquot of concentrated CNZ in acidic solution (i.e., the “spring”) was added to present an initial concentration of 20 µg/ml and then the solution concentration was evaluated as a function of time.

The equilibrium solubility of CNZ in alkaline solution was measured to be 2 µg/ml, so alkaline solution was spiked to attain an initial supersaturation ratio of 10. The rationale for the relatively low excipient concentration

(0.04% w/v) used throughout supersaturation test indicates that even very low concentrations of excipient (in the same range as the 0.04% used in this study) may be adequate to efficiently inhibit precipitation.<sup>10,11</sup> The concentration-time profiles after the creation of supersaturation in alkaline solution are illustrated in Figure 1. As shown in this Figure, in absence of excipient, the CNZ concentration reduces quickly until it reaches concentration close to the equilibrium solubility of CNZ. This fast decline in CNZ concentration proposes that CNZ precipitated from the supersaturated solution rapidly. Similar findings have been published previously wherein felodipine and celecoxib immediately precipitated in the absence of additives.<sup>12,13</sup>

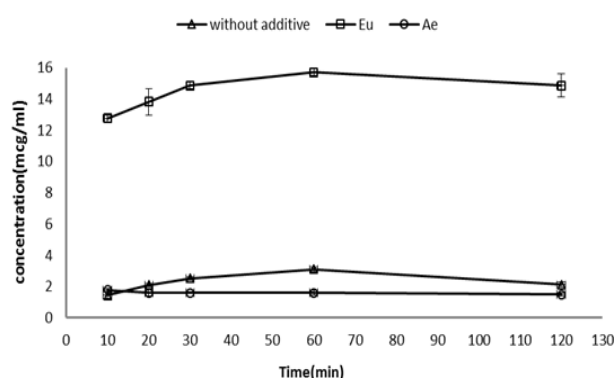


**Figure 1.** Inhibitory effects of Eu and Ae on precipitation of a supersaturated solution of CNZ (20 µg/ml) at pH 6.8.

In the presence of Eu, CNZ concentration determined 20 min after addition of a concentrated solution of CNZ, was remarkably higher than without polymer. The CNZ concentration determined after 20 min was almost 14 µg/mL for 0.04% w/v Eu concentration. After 120 min, CNZ maintained the concentration of 14 µg/mL in Eu solution. According to the results, no significant difference was found between the equilibrium solubility of CNZ in Eu solution ( $2.13 \pm 0.08$  µg/ml) and non-polymer solution ( $2.07 \pm 0.07$  µg/ml) ( $p > 0.05$ ). This implies that Eu has no solubilization effect, and reveals that supersaturated state of the drug in the presence of Eu is attributed to the inhibition effect of the Eu on CNZ

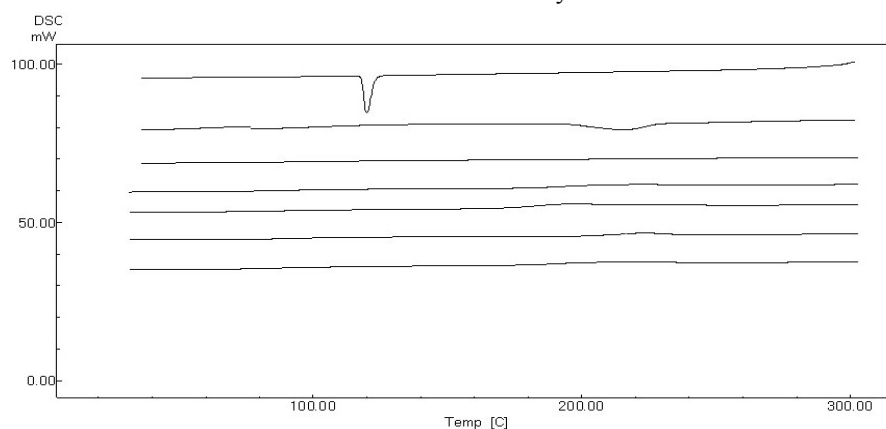


**Figure 2.** DSC scans of the samples from up to down: plain CNZ, Eu, Ae, CNZ loaded Ae (1:5), CNZ loaded Ae (1:15), CNZ-Eu coloaded Ae (1:5:2.5) and CNZ loaded Ae (1:5) after 3 month.

precipitation. When Ae was pre-dispersed in a buffer solution, this affected CNZ supersaturation negatively. Surprisingly, rather than beginning a steady decrease of the supersaturation, the presence of Ae led to a rapid decline of the supersaturation. It could be assumable that the presence of colloidal particles of Ae interrupts the stable supersaturation of CNZ. This result may also be attributed to the adsorption of some CNZ on the surface of Ae because of the absorptive nature of Ae.

### Physical characterization of the CNZ loaded Ae formulations

The DSC thermograms of plain CNZ, Ae, Eu, CNZ loaded Ae and CNZ-Eu co-loaded Ae are represented in Figure 2. Plain CNZ melts at 119.8°C. However, there was no crystalline peak found in the DSC curves of Ae and Eu implying their amorphous states. In the case of the CNZ loaded Ae, contrary to plain CNZ, no endothermic peak was observed suggesting that CNZ was dispersed in the CNZ loaded Ae formulation at a molecular level or amorphous state. This obviously implied that CNZ effectively was adsorbed in the internal pores of Ae. As it was expected, in the DSC thermogram of CNZ-Eu co-loaded Ae formulation, no melting peak of CNZ was seen. Even after 3 months, the CNZ:Ae based formulations did not show any signs of crystallinity, providing evidence for the good physical stability of CNZ loaded Ae formulations. This may be related to the adsorption effect of Ae which inhibited crystallization of the drug in drug /Ae composition. Similar findings have been reported in previous investigations.<sup>11,14</sup> To investigate a possible interaction between CNZ and Ae, the FT-IR spectra of pure CNZ and CNZ loaded Ae were determined (Figure 3). The pure CNZ has bands at 3066  $\text{cm}^{-1}$  (aromatic CH stretch), 3021  $\text{cm}^{-1}$  (alkene CH stretch), 2956  $\text{cm}^{-1}$  (aliphatic CH stretch), 1141  $\text{cm}^{-1}$  (C-N stretch), 1001  $\text{cm}^{-1}$  (=C-H alkene) and 963  $\text{cm}^{-1}$  (=C-H aromatic).<sup>15</sup> The FT-IR spectrum of Ae exposed a band at 3448  $\text{cm}^{-1}$  which can be related to OH resulting from hydrogen bonding between silica oxygen and water (from moisture or crystallization) and or generation of chelate compositions. The peak at about 1637  $\text{cm}^{-1}$  matches to H-O-H bending of crystallization water.

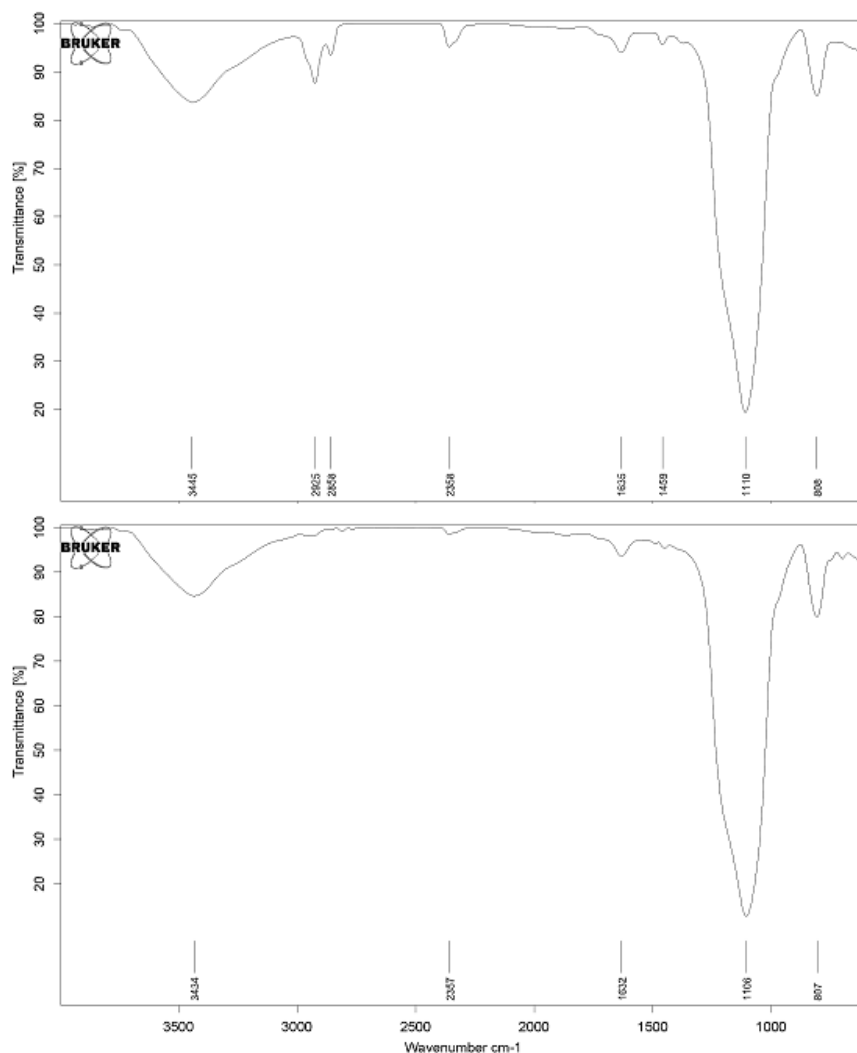


**Figure 3.** FT-IR of spectrum of samples (up) Ae, (down) CNZ loaded Ae.

Moreover, Ae has bands at approximately  $1110\text{ cm}^{-1}$  (the Si-O symmetric stretching vibration),  $810\text{ cm}^{-1}$  (asymmetric Si-O stretching) and  $474\text{ cm}^{-1}$  (Si-O bending modes). Similar spectrum has been previously reported for Ae.<sup>16,17</sup> Interactions were observed between CNZ and Ae illustrated by shifting ( $4\text{ cm}^{-1}$ ) in the symmetric stretching Si-O band of Ae at  $1110\text{ cm}^{-1}$  to  $1106\text{ cm}^{-1}$ . It could be supposed that this interaction may immobilize CNZ molecules preventing them from nucleation and crystallization.<sup>18,19</sup> The small shift of  $4\text{ cm}^{-1}$  for the Si-O band demonstrated a relatively weak interaction between CNZ and Ae. This is advantageous because a strong interaction could hinder the drug release from the CNZ-loaded Ae formulations.

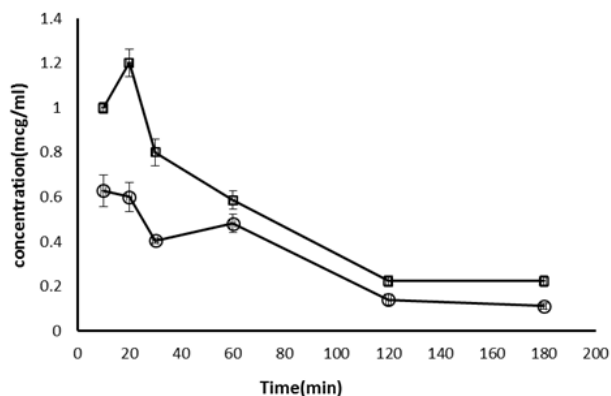
#### ***Effect of loading of CNZ onto Ae on drug dissolution***

The dissolution profiles of plain CNZ and the release profiles for CNZ loaded Ae samples are illustrated in Figure 4. From this Figure it is obvious that, as expected based on the solid-state characteristics of the loaded CNZ, the release from the CNZ loaded Ae was quicker than the dissolution of the crystalline CNZ. Similar results have

been reported in previous investigations.<sup>20,21</sup> The fast drug release from CNZ loaded Ae may be explained by both higher specific surface area of CNZ due to loading into Ae and possibly changing solid state of the drug from crystalline to amorphous state.<sup>22,23</sup> The loaded drug serves the marked decrease in particle size of drug and consequently the strong increase in its surface area. According to the Noyes–Whitney equation, there is a direct correlation between the surface area of drug and dissolution rate of the drug. Moreover, in the amorphous state, no energy is needed to break up crystal arrangements before the dissolution of the drug.<sup>24</sup> In spite of higher initial drug concentration, after 60 minutes, CNZ concentration in solution had fallen from 1.20 to  $0.58\text{ }\mu\text{g/mL}$  for CNZ loaded Ae at CNZ/Ae 20:200 ratio. This is because of this fact that CNZ is rapidly released from the Ae while the released CNZ are prone to precipitation.

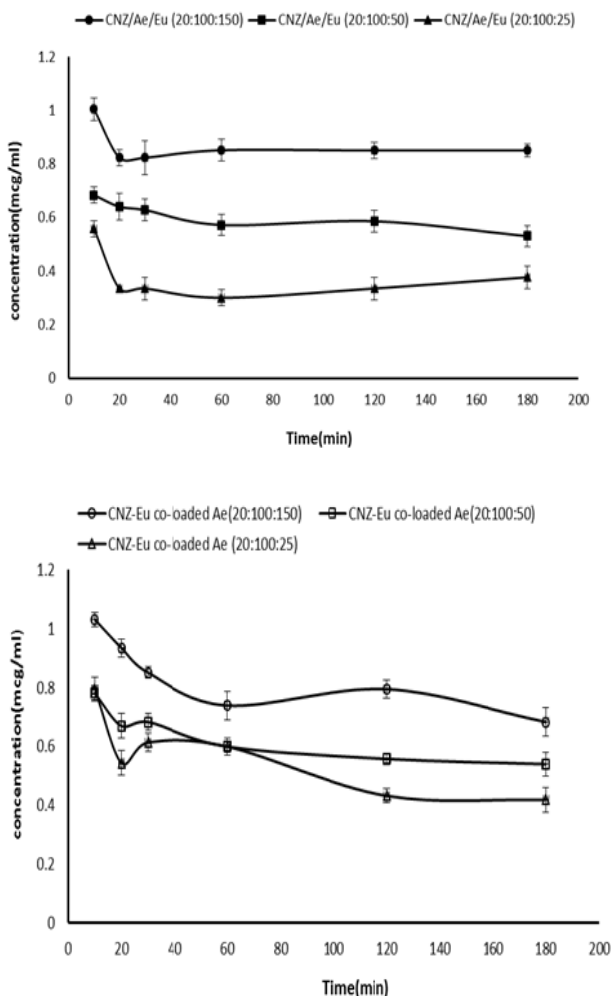
#### ***Effect of CNZ/Ae/Eu ratio on drug dissolution***

Figure 5 shows the effect of Eu on the dissolution performance of CNZ loaded Ae formulations.



**Figure 4.** In vitro release of CNZ (o) and CNZ loaded Ae (CNZ/Ae 20:200) (□)

It is obvious that the physical addition of Eu to CNZ loaded Ae resulted in higher CNZ concentrations. Up to 180 min, concentrations in solution remained significantly higher in the presence of Eu. Addition of Eu to CNZ loaded Ae formulation improved the dissolution performance of the formulation because the co-dissolved Eu inhibited CNZ precipitation, whereas in the absence of Eu the released CNZ from Ae was precipitated quickly.



**Figure 5.** In vitro release of up: CNZ loaded Ae blended with Eu at different CNZ/ Eu ratios and down: CNZ-Eu co-loaded Ae at different CNZ/Eu ratios.

This effect of Eu was according to the results of supersaturation tests (Figure 1). The CNZ –loaded Ae formulations with a different combination of Ae and Eu was examined. Figure 5 shows the dissolution profiles of CNZ from both Eu –CNZ co-loaded Ae and CNZ loaded Ae blended with Eu formulations containing various amount of Eu (CNZ/Ae/Eu ratios 20:100:25, 20:100:50 and 20:100:150).

This Figure revealed that an increase in the amount of Eu blended with CNZ loaded Ae resulted in a significant increase in the dissolution performance. This may be related to more marked precipitation inhibition as a consequence of higher Eu concentration. For example, the relative CNZ concentration after 180 min amounted to 0.37 and 0.9 µg/ml for formulations with 25 and 150 mg Eu, respectively.

Comparison of the drug profiles from Eu –CNZ co-loaded Ae with the drug profiles from CNZ loaded Ae blended with Eu showed that co-loading of Eu with CNZ, had approximately the same effect on drug release as physical blending with CNZ loaded Ae. In both formulations, the higher Eu concentration led to higher CNZ concentration and formulations containing 150 mg Eu provided the highest AUC, both for Eu –CNZ co-loaded Ae and CNZ loaded Ae blended with Eu (Table 1).

**Table 1.** The area under the dissolution curve (AUC) for different formulations.

Samples with different CNZ/Ae/Eu ratios	AUC (µg.min/ml)	
	CNZ loaded Ae blended with EU	CNZ-Eu co-loaded Ae
CNZ/Ae/Eu(20:100:25)	81.9±5.4	87.1±6.3
CNZ/Ae/Eu(20:100:50)	105.9±6.0	100.1±4.2
CNZ/Ae/Eu(20:100:150)	157.4±8.4	132.4±6.1
CNZ/Ae/Eu(20:100:50)	105.9±6.0	100.1±4.2
CNZ/Ae/Eu(20:200:50)	145.6±4.5	110.4±3.2
CNZ/Ae/Eu(20:300:50)	146.3±3.4	127.3±2.9

According to results, the addition of less than 150 mg of Eu led to similar AUC, both for Eu –CNZ co-loaded Ae and CNZ loaded Ae blended with Eu, however, 150 mg Eu improves the AUC much less for the former. This could be attributed to the covering of CNZ particles by high quantity Eu in this formulation, which hinders the penetration of the dissolution medium into the pores of Ae and/or decreases the direct contact of the CNZ with media.

Figure 6 presents the dissolution profiles of CNZ from both Eu –CNZ co-loaded Ae and CNZ loaded Ae blended with Eu formulations containing various amount of Ae (CNZ/Ae/Eu ratios 20:100:50, 20:200:50 and 20:300:50). As it was expected, increasing the amount of Ae led to a significant increase in dissolution performance.

The enhanced CNZ concentrations for CNZ loaded Ae blended with Eu formulation at CNZ/Ae/Eu 20:200:50 ratio over CNZ/Ae/Eu 20:100:50 ratio may simply be related to the higher amount of Ae, providing a more increasing in drug surface area, as discussed previously. However, as can be seen from Figure 6, a direct correlation between the Ae amount and the drug concentration was not obtained. The CNZ concentration

for CNZ loaded Ae blended with Eu at CNZ/Ae/Eu 20:300:50 ratio and CNZ/Ae/Eu 20:200:50 ratio was relatively similar, while sample at CNZ/Ae/Eu 20:100:50 ratio differed with a lower concentration of CNZ. This proposed that the promotion effect of Ae was not proportional to its amount, but rather there was an optimal amount where the increase in the drug concentration was highest.

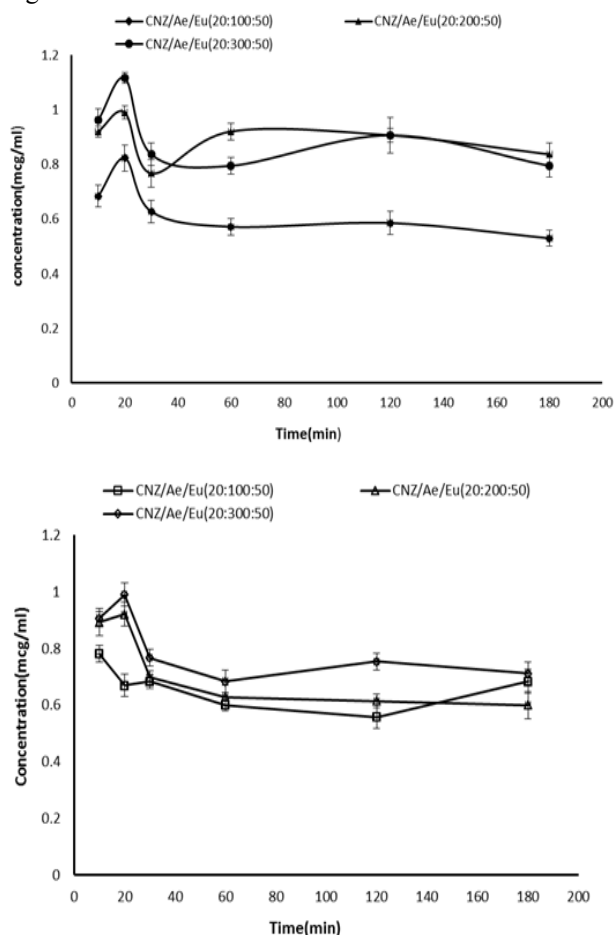


**Figure 6.** In vitro release of up: CNZ loaded Ae blended with Eu at different CNZ/Ae ratios and down: CNZ-Eu co-loaded Ae at different CNZ/Ae ratios.

AUC statistical analysis also demonstrated no significant difference among CNZ loaded Ae blended with Eu at CNZ/Ae/Eu 20:300:50 ratio and CNZ/Ae/Eu 20:200:50 ratio ( $p < 0.05$ ) (Table 1). Both samples provide an AUC improvement of almost 1.5 fold of plain CNZ (AUC=50  $\mu\text{g}\cdot\text{min}/\text{ml}$ ). CNZ loaded Ae blended with Eu at CNZ/Ae/Eu 20:200:50 ratio was chosen as the most promising sample for getting the highest CNZ concentration, with the greatest CNZ loading and lowest Ae content. Comparing the Eu-CNZ co-loaded Ae samples with the CNZ loaded Ae blended with Eu samples revealed that the promotion effect of Ae on drug concentration was less pronounced in the former because of the hindering effect of Eu on the dissolution of the drug in these samples.

### Conclusion

According to the obtained results, even though Ae was

capable of increasing CNZ dissolution rate, its effect was limited as a consequence of precipitation of the released drug. The polymer Eu was found to be an efficient precipitation inhibitor of CNZ, and physically blending of Eu with CNZ-loaded Ae led to a more pronounced effect compared to the co-loading of Eu and CNZ onto Ae. This work has revealed that incorporation of Ae and an efficient precipitation inhibitor provides a valuable approach to improve the *in vitro* dissolution performance of poorly water-soluble drugs.

### Acknowledgements

The financial support from Drug Applied Research Center of Tabriz University of Medical Sciences is greatly acknowledged.

### Conflict of interests

The authors claim that there is no conflict of interest.

### References

- Shen SC, Ng WK, Chia LS, Dong YC, Tan RB. Applications of mesoporous materials as excipients for innovative drug delivery and formulation. *Curr Pharm Des.* 2013;19(35):6270-89. doi:10.2174/1381612811319350005
- Vialpando M, Martens JA, Van den Mooter G. Potential of ordered mesoporous silica for oral delivery of poorly soluble drugs. *Ther Deliv.* 2011;2(8):1079-91. doi:10.4155/tde.11.66
- Xu W, Riikonen J, Lehto VP. Mesoporous systems for poorly soluble drugs. *Int J Pharm.* 2013;453(1):181-97. doi:10.1016/j.ijpharm.2012.09.008
- Van Speybroeck M, Barillaro V, Thi TD, Mellaerts R, Martens J, Van Humbeeck J, et al. Ordered mesoporous silica material SBA-15: a broad-spectrum formulation platform for poorly soluble drugs. *J Pharm Sci.* 2009;98(8):2648-58. doi:10.1002/jps.21638
- Shen SC, Ng WK, Chia L, Dong YC, Tan RB. Stabilized amorphous state of ibuprofen by co-spray drying with mesoporous SBA-15 to enhance dissolution properties. *J Pharm Sci.* 2010;99(4):1997-2007. doi:10.1002/jps.21967
- Mellaerts R, Houthoofd K, Elen K, Chen H, Van Speybroeck M, Van Humbeeck J, et al. Aging behavior of pharmaceutical formulations of itraconazole on SBA-15 ordered mesoporous silica carrier material. *Microporous Mesoporous Mater.* 2010;130(1-3):154-61. doi:10.1016/j.micromeso.2009.10.026
- Guzmán HR, Tawa M, Zhang Z, Ratanabangkoon P, Shaw P, Gardner CR, et al. Combined use of crystalline salt forms and precipitation inhibitors to improve oral absorption of celecoxib from solid oral formulations. *J Pharm Sci.* 2007;96(10):2686-702. doi:10.1002/jps.20906
- Gao P, Rush BD, Pfund WP, Huang T, Bauer JM, Morozowich W, et al. Development of a supersaturable SEDDS (S-SEDDS) formulation of

- paclitaxel with improved oral bioavailability. *J Pharm Sci.* 2003;92(12):2386-98. doi:10.1002/jps.10511
9. Gao P, Guyton ME, Huang T, Bauer JM, Stefanski KJ, Lu Q. Enhanced oral bioavailability of a poorly water soluble drug PNU-91325 by supersaturatable formulations. *Drug Dev Ind Pharm.* 2004;30(2):221-9. doi:10.1081/DDC-120028718
  10. Gao P, Akrami A, Alvarez F, Hu J, Li L, Ma C, et al. Characterization and optimization of AMG517 supersaturatable self-emulsifying drug delivery system (S-SEDDS) for improved oral absorption. *J Pharm Sci.* 2009;98(2):516-28. doi:10.1002/jps.21451
  11. Van Speybroeck M, Mols R, Mellaerts R, Thi TD, Martens JA, Van Humbeeck J, et al. Combined use of ordered mesoporous silica and precipitation inhibitors for improved oral absorption of the poorly soluble weak base itraconazole. *Eur J Pharm Biopharm.* 2010;75(3):354-65. doi:10.1016/j.ejpb.2010.04.009
  12. Abu-Diak OA, Jones DS, Andrews GP. An investigation into the dissolution properties of celecoxib melt extrudates: understanding the role of polymer type and concentration in stabilizing supersaturated drug concentrations. *Mol Pharm.* 2011;8(4):1362-71. doi:10.1021/mp200157b
  13. Konno H, Handa T, Alonzo DE, Taylor LS. Effect of polymer type on the dissolution profile of amorphous solid dispersions containing felodipine. *Eur J Pharm Biopharm.* 2008;70(2):493-9. doi:10.1016/j.ejpb.2008.05.023
  14. Jia Z, Lin P, Xiang Y, Wang X, Wang J, Zhang X, et al. A novel nanomatrix system consisted of colloidal silica and pH-sensitive polymethylacrylate improves the oral bioavailability of fenofibrate. *Eur J Pharm Biopharm.* 2011;79(1):126-34. doi:10.1016/j.ejpb.2011.05.009
  15. Haress NG. Cinnarizine: Chapter One - Cinnarizine: Comprehensive Profile. In: Harry GB, editor. *Profiles of Drug Substances, Excipients and Related Methodology.* Waltham: Academic Press; 2015. P.1-41.
  16. Rus LM, Tomuta I, Iuga C, Maier C, Kacso I, Borodi G, et al. Compatibility studies of indapamide/pharmaceutical excipients used in tablet preformulation. *Farmacia.* 2012;60(1):92-101.
  17. El-Gizawy SA, Osman MA, Arafat MF, El Maghraby GM. Aerosil as a novel co-crystal co-former for improving the dissolution rate of hydrochlorothiazide. *Int J Pharm.* 2015;478(2):773-8. doi:10.1016/j.ijpharm.2014.12.037
  18. Bhugra C, Pikal MJ. Role of thermodynamic, molecular, and kinetic factors in crystallization from the amorphous state. *J Pharm Sci.* 2008;97(4):1329-49. doi:10.1002/jps.21138
  19. Lipp R. Selection and use of crystallization inhibitors for matrix-type trans-dermal drug-delivery systems containing sex steroids. *J Pharm Pharmacol.* 1998;50(12):1343-9. doi:10.1111/j.2042-7158.1998.tb03357.x
  20. Zhang P, Forsgren J, Strømme M. Stabilisation of amorphous ibuprofen in Upsalite, a mesoporous magnesium carbonate, as an approach to increasing the aqueous solubility of poorly soluble drugs. *Int J Pharm.* 2014;472(1-2):185-91. doi:10.1016/j.ijpharm.2014.06.025
  21. Zhang P, Zardán Gómez de la Torre T, Forsgren J, Bergström CAS, Strømme M. Diffusion-controlled drug release from the mesoporous magnesium carbonate Upsalite®. *J Pharm Sci.* 2016;105(2):657-63. doi:10.1002/jps.24553
  22. Hu Y, Wang J, Zhi Z, Jiang T, Wang S. Facile synthesis of 3D cubic mesoporous silica microspheres with a controllable pore size and their application for improved delivery of a water-insoluble drug. *J Colloid Interface Sci.* 2011;363(1):410-7. doi:10.1016/j.jcis.2011.07.022
  23. Hu Y, Zhi Z, Wang T, Jiang T, Wang S. Incorporation of indomethacin nanoparticles into 3-D ordered macroporous silica for enhanced dissolution and reduced gastric irritancy. *Eur J Pharm Biopharm.* 2011;79(3):544-51. doi:10.1016/j.ejpb.2011.07.001
  24. Leuner C, Dressman J. Improving drug solubility for oral delivery using solid dispersions. *Eur J Pharm Biopharm.* 2000;50(1):47-60. doi:10.1016/S0939-6411(00)00076-x